

On Vectorization of Deep Convolutional Neural Networks for Vision Tasks

Jimmy S.J. Ren Li Xu

Lenovo Research & Technology

<http://vcnn.deeplearning.cc>

jimmy.sj.ren@gmail.com xulihk@lenovo.com

Abstract

We recently have witnessed many ground-breaking results in machine learning and computer vision, generated by using deep convolutional neural networks (CNN). While the success mainly stems from the large volume of training data and the deep network architectures, the vector processing hardware (e.g. GPU) undisputedly plays a vital role in modern CNN implementations to support massive computation. Though much attention was paid in the extent literature to understand the algorithmic side of deep CNN, little research was dedicated to the vectorization for scaling up CNNs. In this paper, we studied the vectorization process of key building blocks in deep CNNs, in order to better understand and facilitate parallel implementation. Key steps in training and testing deep CNNs are abstracted as matrix and vector operators, upon which parallelism can be easily achieved. We developed and compared six implementations with various degrees of vectorization with which we illustrated the impact of vectorization on the speed of model training and testing. Besides, a unified CNN framework for both high-level and low-level vision tasks is provided, along with a vectorized Matlab implementation with state-of-the-art speed performance.

Introduction

Deep convolutional neural network (CNN) has become a keen tool in addressing large scale artificial intelligence tasks. Though the study of CNN can be traced back to late 1980s (LeCun et al. 1989; LeCun et al. 1990), the recent success of deep CNN is largely attributed to the concurrent progresses of the two technical streams. On the one hand, the new deep CNN architecture with elements such as Dropout (Hinton et al. 2012; Krizhevsky, Sutskever, and Hinton 2012), DropConnect (Wan et al. 2013), Rectified Linear Units-ReLU (Nair and Hinton 2010) as well as new optimization strategies (Dean et al. 2012) have empowered deep CNN with greater learning capacity. On the other hand, the rapid advances and democratization of high performance general purpose vector processing hardware, typified by graphics

processing unit (GPU), unleashes the potential power of deep CNN by scaling up the network significantly.

Various infrastructures were used in scaling up deep CNNs, including GPU (Coates et al. 2013), distributed CPU based framework (Dean et al. 2012), FPGA (Farabet et al. 2009), etc. Though the implementation details among those approaches differ, the core insight underlying the idea of scaling up deep CNN is parallelization (Bengio and LeCun 2007) in which vectorization technique is the fundamental element. While the consecutive distinguished performance of GPU trained CNNs in the ImageNet visual recognition challenge (Krizhevsky, Sutskever, and Hinton 2012; Russakovsky et al. 2013) as well as the reported results in many studies in the literature justify its effectiveness (Jia et al. 2014; Sermanet et al. 2013), the published literature did not provide sufficient insights on how the vectorization was carried out in detail. We also found there is no previous study to answer how different degrees of vectorization influence the performance of deep CNN, which is, however, crucial in finding the bottlenecks and helps to scale up the network architecture. We believe these questions form a significant research gap and the answer to these questions shall shed some light on the design, tuning and implementation of vectorized CNNs.

In this paper, we reinterpret the key operators in deep CNNs in vectorized forms with which high parallelism can be easily achieved given basic parallelized matrix-vector operators. To show the impact of the vectorization on the speed of both model training and testing, we developed and compared six implementations of CNNs with various degrees of vectorization. We also provide a unified framework for both high-level and low-level vision applications including recognition, detection, denoise and image deconvolution. Our Matlab Vectorized CNN implementation (VCNN) will be made publicly available on the project webpage.

Related Work

Efforts on speeding up CNN by vectorization starts with its inception. Specialized CNN chip (Jackel et al. 1990) was built and successfully applied to handwriting recognition in the early 90s. Simard et al. (2003) simplified CNN by fusing convolution and pooling operations. This speeded up the network and performed well in document analysis. Chellapilla

et al. (2006) adopted the same architecture but unrolled the convolution operation into a matrix-matrix product. It has now been proven that this vectorization approach works particularly well with modern GPUs. However, limited by the available computing power, the scale of the CNN explored at that time was much smaller than modern deep CNNs.

When deep architecture showed its ability to effectively learn highly complex functions (Hinton, Osindero, and Teh 2006), scaling up neural network based models was soon becoming one of the major tasks in deep learning (Bengio and LeCun 2007). Vectorization played an important role in achieving this goal. Scaling up CNN by vectorized GPU implementations such as Caffe (Jia et al. 2014), Overfeat (Sermanet et al. 2013), CudaConvnet (Krizhevsky, Sutskever, and Hinton 2012) and Theano (Bergstra et al. 2010) generates state-of-the-art results on many vision tasks. Albeit the good performance, few of the previous papers elaborated on their vectorization strategies. As a consequence, how vectorization affects design choices in both model training and testing is unclear.

Efforts were also put in the acceleration of a part of the deep CNN from algorithmic aspects, exemplified by the separable kernels for convolution (Denton et al. 2014) and the FFT speedup (Mathieu, Henaff, and LeCun 2013). Instead of finding a faster alternative for one specific layer, we focus more on the general vectorization techniques used in *all* building blocks in deep CNNs, which is instrumental not only in accelerating existing networks, but also in providing guidance for implementing and designing new CNNs across different platforms, for various vision tasks.

Vectorization of Deep CNN

Vectorization refers to the process that transforms the original data structure into a vector representation so that the scalar operators can be converted into a vector implementation. In this section, we introduce vectorization strategies for different layers in Deep CNNs.

Figure 1 shows the architecture of a typical deep CNN for vision tasks. It contains all of the essential parts of modern CNNs. Comprehensive introductions on CNN’s general architecture and the recent advances can be found in (LeCun et al. 1998) and (Krizhevsky, Sutskever, and Hinton 2012).

We mark the places where vectorization plays an important role. “**a**” is the convolution layer that transforms the input image into feature representations, whereas “**b**” is the one to handle the pooling related operations. “**c**” represents the convolution related operations for feature maps. We will see shortly that the vectorization strategies between “**a**” and “**c**” are slightly different. “**d**” involves operations in the fully connected network. Finally, “**e**” is the vectorization operation required to simultaneously process multiple input samples (e.g. mini-batch training). It is worth noting that we need to consider both forward pass and back-propagation for all these operations.

Vectorizing Convolution

We refer to the image and intermediate feature maps as f , one of the convolution kernels as w_i , the convolution layer

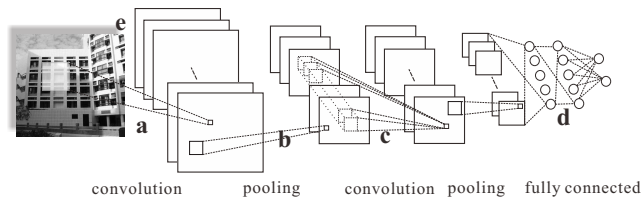


Figure 1: Convolutional Neural Network architecture for visual recognition.

can be typically expressed as

$$f_i^{l+1} = \sigma(w_i^l * f^l + b_i^l), \quad (1)$$

where i indexes the i^{th} kernel. l indexes the layer. b^l is the bias weight. $*$ is the convolution operator. For vision tasks, f can be 2- or 3-dimension. The outputs from previous layer can be deemed as one single input f^l . σ is the nonlinear function which could be ReLU, hyperbolic tangent, sigmoid, etc. Adding bias weight and applying nonlinear mapping are element-wise operations which can be deemed as already fully vectorized, i.e. the whole feature vector can be processed simultaneously. Contrarily, the convolution operators involve a bunch of multiplication with conflict memory access. Even the operators are parallelized for each pixel, the parallelism (Ragan-Kelley et al. 2013) to be exploited is rather limited: compared to the number of computing units on GPU, the number of convolution in one layer is usually smaller. A fine-grained parallelism on element-wise multiplication is much preferred, leading to the vectorization process to unroll the convolution.

In what follows, all the original data f , b and w can be viewed as data vectors. Specifically, we seek vectorization operators $\varphi_c()$ to map kernel or feature map to its matrix form so that convolution can be conducted by matrix-vector multiplication. However, a straight forward kernel-matrix, image-vector product representation of convolution is not applicable here, since the kernel matrix is a sparse block-Toeplitz-Toeplitz-block one, not suitable for parallelization due to the existence of many zero elements. Thanks to the duality of kernel and feature map in convolution, we can construct a *dense* feature-map-matrix and a kernel-vector. Further, multiple kernels can be put together to form a matrix so as to generate multiple feature map outputs simultaneously,

$$[f_i^{l+1}]_i = \sigma(\varphi_c(f^l)[w_i^l]_i + [b_i^l]_i). \quad (2)$$

Operator $[]_i$ is to assemble vectors with index i to form a matrix.

Backpropagation The training procedure requires the backward propagation of gradients through $\varphi_c(f^l)$. Note that $\varphi_c(f^l)$ is in the unrolled matrix form, different from the outputs of previous layer $[f_i^l]_i$. An inverse operator $\varphi_c^{-1}()$ is thus required to transform the matrix-form gradients into the vector form for further propagation. Since $\varphi_c()$ is a one-to-many mapping, $\varphi_c^{-1}()$ is a many-to-one operator. Fortunately, the gradient update is a linear process which can also be processed separately and combined afterwards.

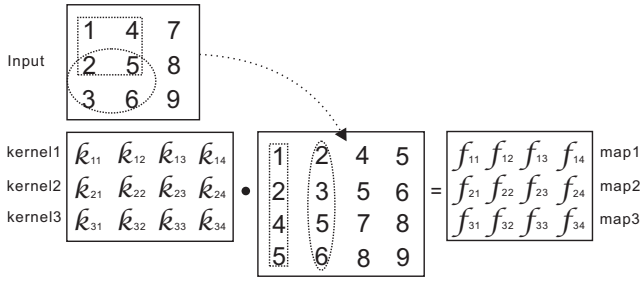


Figure 2: Strategy to vectorize convolution. Illustration of the way to convolve a 3x3 input image with three 2x2 kernels and generates three 2x2 feature maps.

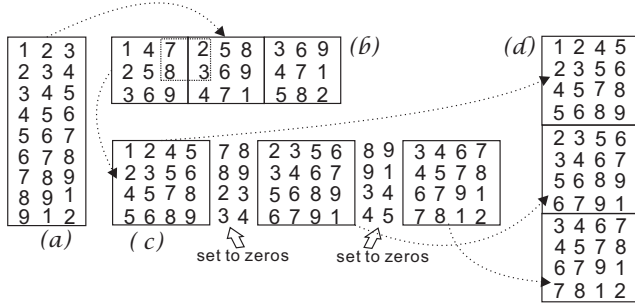


Figure 3: Strategy to vectorize convolution with a feature map. Illustration of the way to convolve a 3x3x3 feature map.

Matlab Practice Our matlab implementation to vectorize the input image is shown in Fig. 2. Specifically, we first crop the image patches base on the kernel size and reorganize them into columns, as indicated by the dotted bounds. Convolution kernels are arranged by rows in another matrix. We can see that the product of these two matrices will put all the convolved feature maps in the resulting matrix, one feature map per row. $\varphi_c()$ here can be efficiently implemented by the `im2col()` functions in Matlab on both GPU¹ and CPU. We note that the feature map vector here are transpose of f_i , simply because the function of `im2col()`.

Convolution with the feature map An alternative practice is needed to handle convolution of the feature map (e.g. “c” in Fig. 1). This is because we need to first combine $[f_i^l]_i$ to a higher dimensional f^l and then perform convolution. One example is illustrated in Fig. 3, where we need to combine $3 \times 3 \times 3$ feature maps to a $3 \times 3 \times 3$ one and apply $\varphi_c()$. In practice, we could first apply three times $\varphi_c()$ to f_i^l and then combine the results. We found it less efficient since the actual number of feature map is much larger. To exploit more parallelism, we try to reorganize the data and apply only once the vectorization operator $\varphi_c()$.

In Fig. 3, we first reshape column vectors $[f_i]_i$ (a) back to a 2D matrix and put them side by side (b). This operation is cheap since it just changes the representation of the data

¹We used a custom version of `im2col()` for GPU.

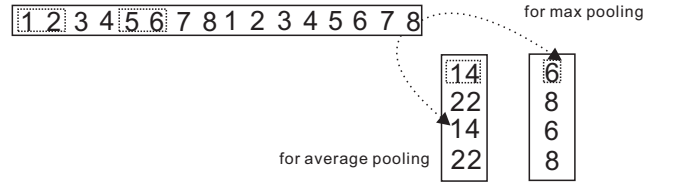


Figure 4: Strategy to vectorize pooling. Illustration of pooling for one 4x4 feature map.

but does not rearrange it. It allows us to vectorize all the feature maps in a holistic way (c). Since only valid region is considered during convolution, we set all the redundant columns to zeros. The final $\varphi_c(f)$ is obtained by rearranging the intermediate result in (c). Since redundant columns are involved, we use Matlab function `accumarray()` to handle many-to-one rearrangement.

One may note that the operator $\varphi_c^{-1}()$ is a many-to-one mapping as well. So it can be efficiently implemented by `accumarray()`, for backpropagation.

Vectorizing Pooling

It is inefficient to carry out the pooling separately for each feature map, so the goal here is to simultaneously process those separate operations by vectorization. The pooling operator can be abstracted as

$$f^{l+1} = \sigma(\varphi_p(f^l) + b^l), \quad (3)$$

where $\varphi_p()$ is a many-to-one mapping with a defined operation corresponding to max- or average- pooling.

Due to the information loss, the inverse operator $\varphi_p^{-1}()$ is not well defined. We simply use nearest neighbor upscaling for approximation during backpropagation.

The pooling operations, both average pooling and max pooling, can be thought of as a vector accumulation process guided by a pre-defined index map, which can be similarly implemented by `accumarray()`. The only difference for max pooling is a `max` function is involved. For overlapping pooling, we could insert the overlapped elements into the feature map and then apply the same pooling strategy.

Vectorizing Fully Connected Layers

The fully connected layers (i.e. “d” in Fig. 1), can be written in a dense matrix-matrix multiplication. Thus both the feed forward and backpropagation are naturally vectorized, in a unified matrix-matrix form.

Vectorization for Mini-batches

Our vectorization strategy can be directly extended to support mini-batch training. Given a batch of samples indexed by j , the mini-batch training with a convolution layer is given by

$$[f_i^{l+1}]_i = \sigma([\varphi_c(f_{:,j}^l)]_j [w_i^l]_i + [b_i^l]_i), \quad (4)$$

where $[]_j$ is to assemble the matrix of different samples.

Figure 5 shows the Matlab implementation of batch mode for the same operation as in Fig. 2 with the batch size of 2.

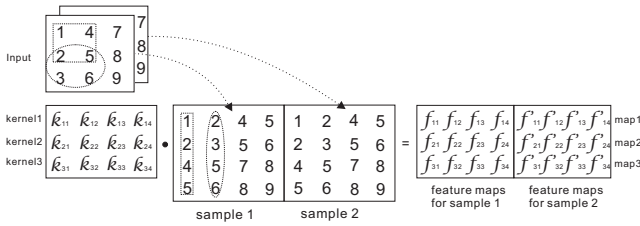


Figure 5: Strategy to vectorize mini-batch operations.

Both samples in the input batch are vectorized and the outputs are arranged horizontally. We can show that the product of the same kernel matrix as in Fig. 2 and this matrix is able to simultaneously generate feature maps for both samples. Note that if an input sample of a convolutional layer has multiple channels, we could treat it as a multi-channel feature map as shown in Fig. 3.

Experiments and Analysis

The goal of the experiments presented in this section is to understand the role of vectorization in training and testing CNNs as well as its limitation.

In order to make our experiment results of high validity and relevancy, we compared the training and testing speed of our fully vectorized implementation with Caffe and Cudaconvnet, the speed is competitive, if not faster in all the tested cases.

Comparing Different Degrees of Vectorization

In this section, we seek to understand the role of vectorization by comparing six CNN implementations. These implementations differ in the degree of vectorization, which is illustrated in table 1. Imp-1 is a least vectorized one, Imp-2 naively parallelize the process of batch samples by adding a parallel for-loop to Imp-1 whilst Imp-6 is a fully vectorized implementation guided by the approaches we introduced. When working with one particular implementation we also observe how results change with network scales. The reason is we would like to examine different vectorization strategies with both small scale network and large scale ones and we are particularly interested in large scale CNNs since it is more relevant to recent advances in the field.

We consider three scales. Scale 1 is a small model, it is very similar to the standard LeNet (LeCun et al. 1998), but with more feature maps in the convolutional layers², ReLU nonlinearity and cross-entropy error. Scale 2 is a large network with about 60 million trainable parameters which is comparable to AlexNet (Krizhevsky, Sutskever, and Hinton 2012). However, the architecture is tailored for the purpose of this study. First, we would like to keep the number of conv layer and the number of fully connected layer balanced so that we shall have a fair performance breakdown. It also allows us to directly compare the results with Scale 1. Second,

²This setting of conv layer is the same in Caffe’s MNIST example. We have 2 fully connected hidden layers.

Vec ele	Fu-co	Conv	Pool	Feat	Batch
Imp-6	✓	✓	✓	✓	✓
Imp-5	✓	✓	✓	✓	
Imp-4	✓	✓	✓		
Imp-3	✓	✓			
Imp-2	✓				✓
Imp-1	✓				

Table 1: Different vectorized elements included in the six CNNs. Fu-co: fully connected layer, Conv: convolutional layer, Pool: pooling layer, Feat: feature map patchification, Batch: vectorize for batch. A tick indicates the element is vectorized

to enable a fair comparison, we would like to have a unified vectorization scheme for convolution throughout the network. Thus unlike AlexNet which uses a stride 4 convolution in the first conv layer and stride 1 thereafter, all convolution operations use the same stride of 1 in our model. The consequences of those are, compare to AlexNet, scale 2 tends to have more feature maps in the conv layer but smaller size for the input images. We set the number of output units to 1000 as in AlexNet. Scale 3 is a larger network with 10,000 output units. This pushes the number of trainable parameters to 94 million, keeping other settings the same as scale 2. The performance on GPU³ (in terms of the number of images to be processed per second) of the six CNNs with different network scales during training is illustrated in table 2.

We are able to observe several insights from the figures. First of all, the results indicates that vectorization is vital to CNN’s speed. We can see that Imp-1 is very slow and a naive parallelization (Imp-2) seems work poorly on GPU. Especially for the large scale networks, Imp-1 and Imp-2 are simply too slow to be practical. When training a small network, a fully vectorized CNN (Imp-6) is more than 200 times faster than the naive parallelization version during training and more than 100 times faster during testing. This acceleration is going to be more significant for bigger networks since Imp-1 and 2 scale poorly.

Second, all vectorization element we introduced contribute significantly to the final performance, during both training and testing. One interesting insight is the contribution of vectorizing pooling and feature map patchification seems to increase with the scale of the network. For instance, in table 2, Imp-4 (vectorize for pooling) has a 1.9x speed up than Imp-3 under scale 1 but a 4.5x speed up and a 4.3x speed up under scale 2 and scale 3 respectively. Same phenomenon happens for testing. This strongly indicates that the vectorization strategy for those two elements scales well with the size of the network.

On the other hand, we also observe that vectorizing batch processing brings more than 10x speed up for small models but only 3x to 5x speed up for large scale models. The contribution of vectorizing batch processing to the performance seems to decrease when scaling up the network though the

³GeForce GTX 780 Ti, same card was used in the rest of the experiments.

#img/sec	Imp-1	Imp-2	Imp-3	Imp-4	Imp-5	Imp-6
Scale 1	1	6.1	15.3	29.5	85.4	1312.1
Scale 2	n/a	n/a	2.4	11	42.3	188.7
Scale 3	n/a	n/a	2.3	10	34.3	161.2

* batch size is 100 for scale 1 and 200 for scale 2 and 3.

Table 2: Training performance of the six CNNs (#images to be processed per second). Scale1: small model, 10 output units; Scale2: large model, 1000 output units, Scale3: larger model, 10000 output units.

speed up remains significant. We further investigate this phenomenon in the next section which leads to a strategy to achieve optimal training and testing speed.

In Search of Optimal Speed

We investigated the puzzle of decelerating speed up by scrutinizing the performance against different batch sizes. The results are presented in table 3 and 4 for training and testing respectively.

#img/sec	b=1	b=100	b=200	b=300	b=400
Scale 1	88.5	1312	1450.9	1574.2	1632.8
Scale 2	41.9	136.9	188.7	192.3	106.3
Scale 3	34.3	123.5	161.3	163.9	91

Table 3: Training performance of Imp-6 against different batch sizes (#images to be processed per second).

#img/sec	b=1	b=100	b=200	b=400	b=600
Scale 1	151.5	1812.6	1878.4	2023.5	2192.2
Scale 2	75.8	222.2	270.2	285.7	103.1
Scale 3	74	212.8	256.4	277.8	89.2

Table 4: Test performance of Imp-6 against different batch sizes (#images to be processed per second).

In table 3, we can see that for the small model (scale 1) the acceleration brought by each adjacent batch size increase is 14x, 1.1x, 1.08x and 1.03x. The acceleration obtained via the increase of batch size seems to be rapidly vanishing. For the large model (scale 2), the first three acceleration ratio are 3.2x, 1.3x and 1.02x, demonstrating the same vanishing trend. Further increase in batch size even leads to a performance degradation instead. Same situation occurs for the larger model (scale 3). Though the ability of processing 192 images/second for training and 285 images/second for testing with our commodity GPU for the scale 2 network is promising, this result still indicates that there is some scaling limitation within the vectorization for batch processing. Similar results in table 4 seems to further suggest that such limitation is shared between training and testing. In order to completely understand the rationale under the hood, we have to resort to a detailed performance breakdown.

Performance Breakdown and Limitation. We decompose the whole training procedure into the following components. They are 1) conv layers; 2) pooling layers; 3) fully connected layers; 4) others (e.g. ReLU, cost). We distinguish

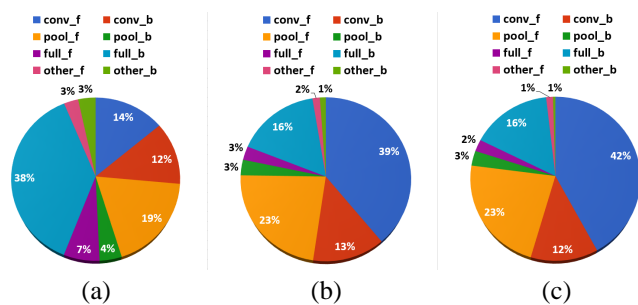


Figure 6: Performance break down. (a) Scale 3 network, batch size = 1. (b) Scale 3 network, batch size = 200. (c) Scale 3 network, batch size = 300. *conv*: conv layers, *pool*: pooling layers, *full*: fully connected layers, *other*: other operations, *f*: forward pass, *b*: back-propagation.

the statistics between forward pass and back-propagation, therefore 8 components to look at.

Figure 6 illustrates the performance break down (in terms of the proportion of computing time in processing one batch) during training of the two representative cases from our largest network (scale 3) in the experiment. Batch size is 1 for Fig. 6(a), 200 for Fig. 6(b) and 300 for Fig. 6(c). We can observe from Fig. 6(a) that 44% of the overall time was used in processing the fully connected layers. It was in fact the biggest consumer of the computing time for this batch size. We also see that the time spent on full_b is significantly more than full_f. This makes sense because it involves larger matrix multiplication and larger transform matrix than that in the forward pass. The second largest consumer of time is the convolution layers and we can see that the time spent in forward pass and back-propagation is reasonably balanced.

However, the situation we found in Fig. 6(b) and Fig. 6(c) is very different. One obvious character is, when increasing the batch size, the time costs by the conv layers is now considerably more than the fully connected layers. While the proportion between full_f and full_b among the three batch sizes roughly remains the same, we found conv_f spent much more time than conv_b for large batch sizes. This indicates the scaling limitation is within the conv_f when vectorizing for batch processing. A further scrutiny on this issue shows that the limitation is caused by the following two factors namely the memory overhead in handling multiple samples and the overhead caused by invoking patchification on bigger samples. While there might be alternative strategies to vectorize batch processing, we argue that the aforementioned overhead is hard to be completely avoided.

Finding the Optimal Speed. We found the observations from Fig. 6 are also valid for scale 1 and scale 2 networks, but with an important difference. For small networks like the scale 1 network, the acceleration brought by batch processing shall be valid for very big batch sizes (e.g. 1000) whilst for large networks batch size needs to be chosen carefully or else the speed degradation like we saw in table 3 and 4 shall occur before the network hits the GPU memory ceiling. This suggests that given a network design choosing an appropriate batch size may be vital in achieving the opti-

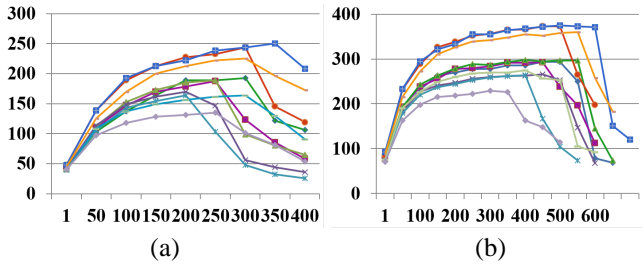


Figure 7: Speed of 10 randomly selected networks. X axis, batch size. Y axis, number of images to be processed per second. (a) for training. (b) for testing.

mal speed. Based on our scale 2 network, we select 10 other networks by randomly adjusting several parameters such as filter size, number of feature maps, number of output units and sigmoid function, etc. We run these networks for both training and testing by adjusting the batch sizes to see if this contention is generally applicable for large networks.

Figure 7 confirms our aforementioned contention for large networks and makes the importance of choosing an appropriate batch size obvious. First, it suggests that the optimal batch size among different network parameters is usually quite different. Directly adopting a batch size from a previous set of network parameters may lead to significantly inferior speed. Second, it also suggests that the optimal batch size between the training stage and the testing stage is also different, even if for the same network. A naive adoption of the batch size from the training stage is often not optimal and leads to considerable speed loss. These findings has direct implications in building real-time systems in which optimization for model testing is the key.

Unification of High/Low Level Vision Tasks

Despite the rapid adoption of deep CNN in addressing various kinds of high level computer vision tasks typified by image classification and object localization, other problems such as detecting objects of different shapes in real-time seem still a problem under investigation. On the other hand, we observed that there are a few very recent studies (Xu et al. 2014; Eigen, Krishnan, and Fergus 2013) successfully used deep CNN in various low level vision tasks such as image deblurring and denoising, etc. Though the domain knowledge required to build those new networks substantially differ from that used in addressing high level vision tasks, same vectorization principles presented in this paper will apply.

More interestingly, the same vectorization principle across those tasks actually gives us a chance (perhaps for the first time) to unify both high level vision tasks and low level vision tasks in a single computational framework. In this section, we introduce the application of our VCNN implementation in tasks seemingly of distinct fields namely, image denoising and deblurring (low level vision) as well as multi-object detection (high level vision).

CNN for Image Processing

Image processing tasks do not require pooling and fully connected layers in general. To verify the effectiveness of the proposed vectorized framework, we implemented a network architecture by simply removing the pooling and fully connected layers from Fig. 1 and trained the network with synthesized clear-noisy image pairs. One of the denoise result is given in Fig. 8. Another sample application of our vectorized CNN is the recent proposed image deconvolution (Xu et al. 2014). Result is shown in Fig. 9.



Figure 8: Application in image denoising.



Figure 9: Application in image deconvolution.

Novel Training Scheme for Multi-object Detection

Conventional image classifiers are usually trained by image samples with equal sizes. This imposes a critical limitation when applying it in detection. For instance, it is reasonable to put a human face sample in a square image, but doing so for non-squared objects (e.g. shoes) tends to include more background content thus introduces more noise which is detrimental to accurate and efficient object detection. One possible alternative is to formulate object detection as a regression problem (Szegedy, Toshev, and Erhan 2013), however, it requires a very large amount of data and usually very big models to capture the variety of the possible patterns.



Figure 10: Application in real time multi-object detection. Shoes review videos are from Youtube.

Using VCNN, we were able to train a single image classifier but with heterogeneous input sizes by using vectorization. The key insight is heterogeneous inputs can actually share all the weights in a CNN except the ones in the connection between conv layer and fully connected layer. This approach not only avoids the background noise but also being a lot more lightweight than the regression approach. We successfully applied it in a detection system which runs in real-time. We can show that this approach tends to have less false alarms and works efficiently with multi-scale detection through vectorization.

Conclusion

In this paper, we elaborate several aspects on vectorization of deep CNN. First, we present the vectorization steps of all essential parts of implementing deep CNNs. The vectorization steps are further exemplified by Matlab practices. Second, we have developed and compared six CNN implementations with different degrees of vectorization to analyze the impact of vectorization on speed. Third, based on the practices, we provide a unified framework for handling both low-level and high-level vision tasks. Experiments on various applications including image denoise, deconvolution and real-time object detection demonstrated the effectiveness of the proposed strategies. As the introduced vectorization techniques are general enough, our future direction includes optimization for different hardware or cloud platforms.

References

- [Bengio and LeCun 2007] Bengio, Y., and LeCun, Y. 2007. Scaling learning algorithms towards ai. *Large-scale kernel machines* 34:1–41.
- [Bergstra et al. 2010] Bergstra, J.; Breuleux, O.; Bastien, F.; Lamblin, P.; Pascanu, R.; Desjardins, G.; Turian, J.; Warde-Farley, D.; and Bengio, Y. 2010. Theano: a cpu and gpu math compiler in python. In *Python in Science Conf*, 1–7.
- [Chellapilla et al. 2006] Chellapilla, K.; Puri, S.; Simard, P.; et al. 2006. High performance convolutional neural networks for document processing. In *International Workshop on Frontiers in Handwriting Recognition*.
- [Coates et al. 2013] Coates, A.; Huval, B.; Wang, T.; Wu, D. J.; Catanzaro, B. C.; and Ng, A. Y. 2013. Deep learning with COTS HPC systems. In *ICML*, 1337–1345.
- [Dean et al. 2012] Dean, J.; Corrado, G.; Monga, R.; Chen, K.; Devin, M.; Le, Q. V.; Mao, M. Z.; Ranzato, M.; Senior, A. W.; Tucker, P. A.; Yang, K.; and Ng, A. Y. 2012. Large scale distributed deep networks. In *NIPS*, 1232–1240.
- [Denton et al. 2014] Denton, E.; Zaremba, W.; Bruna, J.; LeCun, Y.; and Fergus, R. 2014. Exploiting linear structure within convolutional networks for efficient evaluation. *arXiv preprint arXiv:1404.0736*.
- [Eigen, Krishnan, and Fergus 2013] Eigen, D.; Krishnan, D.; and Fergus, R. 2013. Restoring an image taken through a window covered with dirt or rain. In *NIPS*.
- [Farabet et al. 2009] Farabet, C.; Poulet, C.; Han, J. Y.; and LeCun, Y. 2009. Cnp: An fpga-based processor for convolutional networks. In *International Conference on Field Programmable Logic and Applications*, 32–37.
- [Hinton et al. 2012] Hinton, G. E.; Srivastava, N.; Krizhevsky, A.; Sutskever, I.; and Salakhutdinov, R. R. 2012. Improving neural networks by preventing co-adaptation of feature detectors. *arXiv preprint arXiv:1207.0580*.
- [Hinton, Osindero, and Teh 2006] Hinton, G.; Osindero, S.; and Teh, Y.-W. 2006. A fast learning algorithm for deep belief nets. *Neural computation* 18(7):1527–1554.
- [Jackel et al. 1990] Jackel, L.; Boser, B.; Denker, J.; Graf, H.; LeCun, Y.; Guyon, I.; Henderson, D.; Howard, R.; Hubbard, W.; and Solla, S. 1990. Hardware requirements for neural-net optical character recognition. In *International Joint Conference on Neural Networks*, 855–861.
- [Jia et al. 2014] Jia, Y.; Shelhamer, E.; Donahue, J.; Karayev, S.; Long, J.; Girshick, R.; Guadarrama, S.; and Darrell, T. 2014. Caffe: Convolutional architecture for fast feature embedding. *arXiv preprint arXiv:1408.5093*.
- [Krizhevsky, Sutskever, and Hinton 2012] Krizhevsky, A.; Sutskever, I.; and Hinton, G. E. 2012. Imagenet classification with deep convolutional neural networks. In *NIPS*, 1106–1114.
- [LeCun et al. 1989] LeCun, Y.; Boser, B.; Denker, J. S.; Henderson, D.; Howard, R. E.; Hubbard, W.; and Jackel, L. D. 1989. Backpropagation applied to handwritten zip code recognition. *Neural computation* 1(4):541–551.
- [LeCun et al. 1990] LeCun, Y.; Boser, B.; Denker, J. S.; Henderson, D.; Howard, R. E.; Hubbard, W.; and Jackel, L. D. 1990. Handwritten digit recognition with a back-propagation network. In *NIPS*.
- [LeCun et al. 1998] LeCun, Y.; Bottou, L.; Bengio, Y.; and Haffner, P. 1998. Gradient-based learning applied to document recognition. *Proceedings of the IEEE* 86(11):2278–2324.
- [Mathieu, Henaff, and LeCun 2013] Mathieu, M.; Henaff, M.; and LeCun, Y. 2013. Fast training of convolutional networks through ffts. *arXiv preprint arXiv:1312.5851*.
- [Nair and Hinton 2010] Nair, V., and Hinton, G. E. 2010. Rectified linear units improve restricted boltzmann machines. In *ICML*, 807–814.
- [Ragan-Kelley et al. 2013] Ragan-Kelley, J.; Barnes, C.; Adams, A.; Paris, S.; Durand, F.; and Amarasinghe, S. 2013. Halide: a language and compiler for optimizing parallelism, locality, and recomputation in image processing pipelines. *ACM SIGPLAN Notices* 48(6):519–530.
- [Russakovsky et al. 2013] Russakovsky, O.; Deng, J.; Huang, Z.; Berg, A. C.; and Fei-Fei, L. 2013. Detecting avocados to zucchinis: What have we done, and where are we going? In *ICCV*, 2064–2071.
- [Sermanet et al. 2013] Sermanet, P.; Eigen, D.; Zhang, X.; Mathieu, M.; Fergus, R.; and LeCun, Y. 2013. Overfeat: Integrated recognition, localization and detection using convolutional networks. *arXiv preprint arXiv:1312.6229*.
- [Simard, Steinkraus, and Platt 2003] Simard, P. Y.; Steinkraus, D.; and Platt, J. C. 2003. Best practices

for convolutional neural networks applied to visual document analysis. In *International Conference on Document Analysis and Recognition*, volume 2, 958–958.

[Szegedy, Toshev, and Erhan 2013] Szegedy, C.; Toshev, A.; and Erhan, D. 2013. Deep neural networks for object detection. In *NIPS*, 2553–2561.

[Wan et al. 2013] Wan, L.; Zeiler, M. D.; Zhang, S.; LeCun, Y.; and Fergus, R. 2013. Regularization of neural networks using dropconnect. In *ICML*, 1058–1066.

[Xu et al. 2014] Xu, L.; Ren, J.; Liu, C.; and Jia, J. 2014. Deep convolutional neural network for image deconvolution. In *NIPS*.